AD

AD-E403 924

Technical Report ARMET-TR-16075

NOSECONE INVERTED-F ANTENNA (IFA) FOR S-BAND TELEMETRY

Aaron Barton

September 2017

U.S. ARMY ARMAMENT RESEARCH, DEVELOPMENT AND ENGINEERING CENTER

Munitions Engineering Technology Center

Picatinny Arsenal, New Jersey

The views, opinions, and/or findings contained in this report are those of the author(s) and should not be construed as an official Department of the Army position, policy, or decision, unless so designated by other documentation.

The citation in this report of the names of commercial firms or commercially available products or services does not constitute official endorsement by or approval of the U.S. Government.

Destroy by any means possible to prevent disclosure of contents or reconstruction of the document. Do not return to the originator.

REPORT DOCUMENTATION PAGE

Form Approved
OMB No. 0704-01-0188

1. REPORT DATE (DD-MM-YYYY)	2. REPORT TYPE	3. DATES COVERED (*From - To*)
September 2017	Final	May 2013 through June 2015

4. TITLE AND SUBTITLE

NOSECONE INVERTED-F ANTENNA (IFA) FOR S-BAND TELEMETRY

5a. CONTRACT NUMBER

5b. GRANT NUMBER

5c. PROGRAM ELEMENT NUMBER

6. AUTHORS

Aaron Barton

5d. PROJECT NUMBER

5e. TASK NUMBER

5f. WORK UNIT NUMBER

7. PERFORMING ORGANIZATION NAME(S) AND ADDRESS(ES)
U.S. Army ARDEC, METC
Fuze & Precision Armaments Technology Directorate
(RDAR-MEF-I)
Picatinny Arsenal, NJ 07806-5000

8. PERFORMING ORGANIZATION REPORT NUMBER

9. SPONSORING/MONITORING AGENCY NAME(S) AND ADDRESS(ES)
U.S. Army ARDEC, ESIC
Knowledge & Process Management (RDAR-EIK)
Picatinny Arsenal, NJ 07806-5000

10. SPONSOR/MONITOR'S ACRONYM(S)

11. SPONSOR/MONITOR'S REPORT NUMBER(S)
Technical Report ARMET-TR-16075

12. DISTRIBUTION/AVAILABILITY STATEMENT
Approved for public release; distribution is unlimited.

13. SUPPLEMENTARY NOTES

14. ABSTRACT

This report summarizes an inverted-F antenna for use in smart munitions and S-band telemetry. Designed to fit within a standard artillery fuze envelope, it can be used in place of a monopole or patch antenna. It requires no external matching components. The measured impedance bandwidth (S11 < -10 dB) is typically 100 MHz. Simulations and measurements of the S11 response and radiation pattern are given with the antenna mounted on a M795 projectile.

15. SUBJECT TERMS
Telemetry Wireless High-G Gun launched DFuze Aerofuze Inverted-F antenna (IFA)
High Frequency Electromagnetic Field Simulation (HFSS)

16. SECURITY CLASSIFICATION OF:			17. LIMITATION OF ABSTRACT	18. NUMBER OF PAGES	19a. NAME OF RESPONSIBLE PERSON
a. REPORT	b. ABSTRACT	c. THIS PAGE			Aaron E. Barton
U	U	U	SAR	23	19b. TELEPHONE NUMBER (Include area code) (973) 724-3521

Standard Form 298 (Rev. 8/98)
Prescribed by ANSI Std. Z39.18

CONTENTS

FIGURES

FIGURES
(continued)

ACKNOWLEDGMENTS

The author would like to thank Dr. Steven Weiss and Theodore K. Anthony (U.S. Army Research Laboratory, Adelphi, MD) for their support with antenna design and simulation using Ansys High Frequency Electromagnetic Field Simulation (HFSS), and John Nickel [U.S. Army Armament Research, Development and Engineering Center (ARDEC), Picatinny Arsenal, NJ] for assistance in performing the anechoic chamber radiation pattern measurements. The author would also like to thank the Precision Munitions Instrumentation Division (U.S. Army ARDEC) staff for their support.

INTRODUCTION

Inverted-F antennas (IFAs) are a popular choice for wireless consumer electronics because they can easily be included as additional artwork on printed circuit boards (PCBs). Numerous design variations exist to facilitate communication standards such as IEEE 802.11 (ref. 1).

Antennas are typically used in artillery, mortar, tank, and other munitions for global positioning system or telemetry capabilities. Since the bodies of munitions are mostly metal, and their outer profile must be maintained for flight characteristics, they provide a more challenging antenna placement problem than typical consumer products whose chassis tend to be made of plastic and can allow for protruding antennas such as monopole whips or blades.

One antenna solution that is commonly used is to place several patch or cavity-backed slot radiators around the body of the munition in a wraparound configuration (refs, 2 and 3). The main lobe of each patch or slot aperture covers an angular sector around the azimuthal plane of the munition. These antennas can either be individual substrates placed in a pocket on the side of the round (refs. 4 and 5), or they can be made on a single curved substrate to form an array that is wrapped around the circumference of the munition (ref. 6). The metal body of the munition acts as the ground plane

Another option is to attempt to cut slots in the body of the munition to form slot antennas. As the slot will affect the structural integrity of the munitions, this option is limited to only high frequency communication links where the slot dimensions can be made small.

Another option is to attempt to integrate antennas on the very extreme ends of the munitions (the nose or the fins) and use the remainder of the projectile as a ground plane. Using the nose usually requires that the nosecone be made of a plastic material to support an embedded monopole, patch (refs. 7 and 8), or scimitar (ref. 9).

ANTENNA DESIGN AND FABRICATION

The designed inverted-F antenna is shown in figure 1, which consists of a radiating element mounted vertically over a circular ground plane. It was originally designed to replace a straight wire monopole. It is embedded in a cavity within an Ultem™ 2300 nosecone, whose outside profile conforms to the North Atlantic Treaty Organization STANAG 2916 fuze standardization agreement. The cavity is filled with Eccostock® FPH and CAT 12-10H filler material for high-G shock survivability. Note that the antenna is located on the center of its ground plane, unlike typical inverted-F antennas found in consumer electronics, which are usually located toward the outer edges of their ground planes.

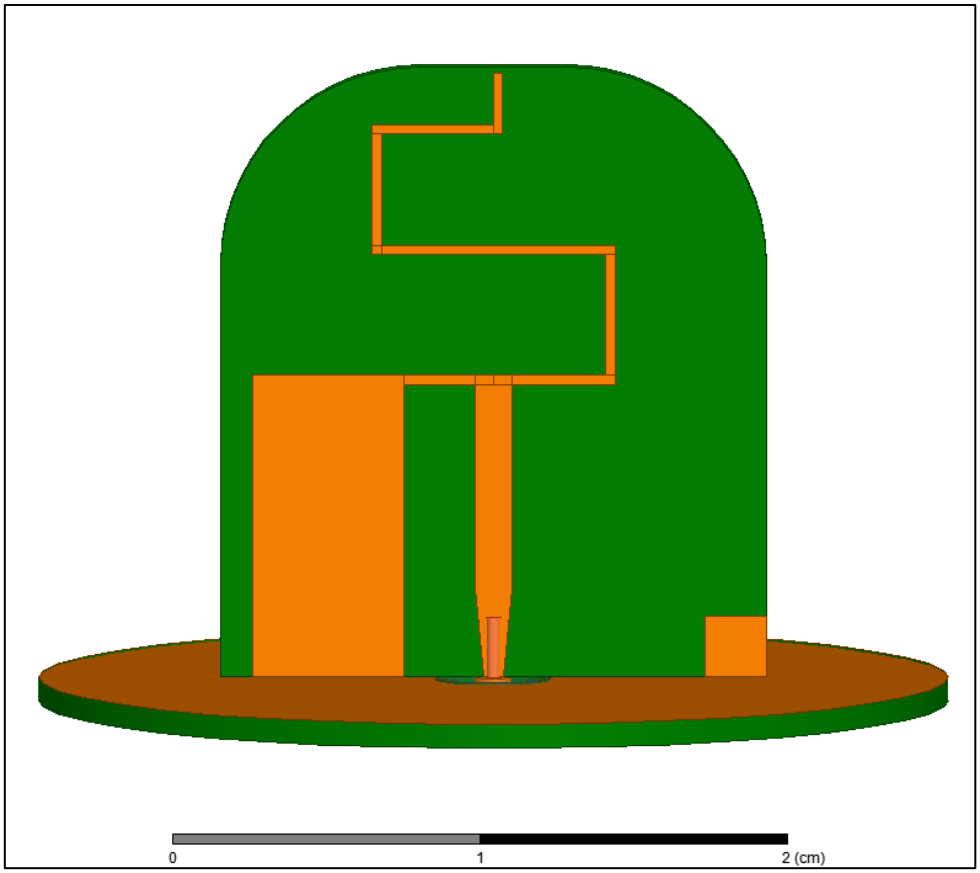

Figure 1
Designed inverted-F antenna (front view)

The antenna is implemented as traces on a pair of FR4 printed circuit boards. The first circuit board is used as a ground plane, and it consists of a circular 0.031-in. FR4 core material with 30-mm outer diameter mounted horizontally. Through holes are provided to support a board-mount coaxial connector. The second circuit board acts as the main antenna radiator and is made of a single-sided 0.031-in. FR4 board mounted vertically. Dimensions of the traces and ground plane are shown in figure 2 and table 1. The IFA includes a 5 by 10-mm ground stub trace, a tapered 1.2 by 10-mm feed trace, and a meandered 0.3-mm trace, whose dimensions were determined experimentally. A feeding probe, extending from the center pin of the coaxial connector, is soldered to the feed trace, which shifts the IFA board slightly off center. The ground plane is soldered to the IFA board at the ground stub and also at a small 2-mm square for mechanical support, as shown in figure 3.

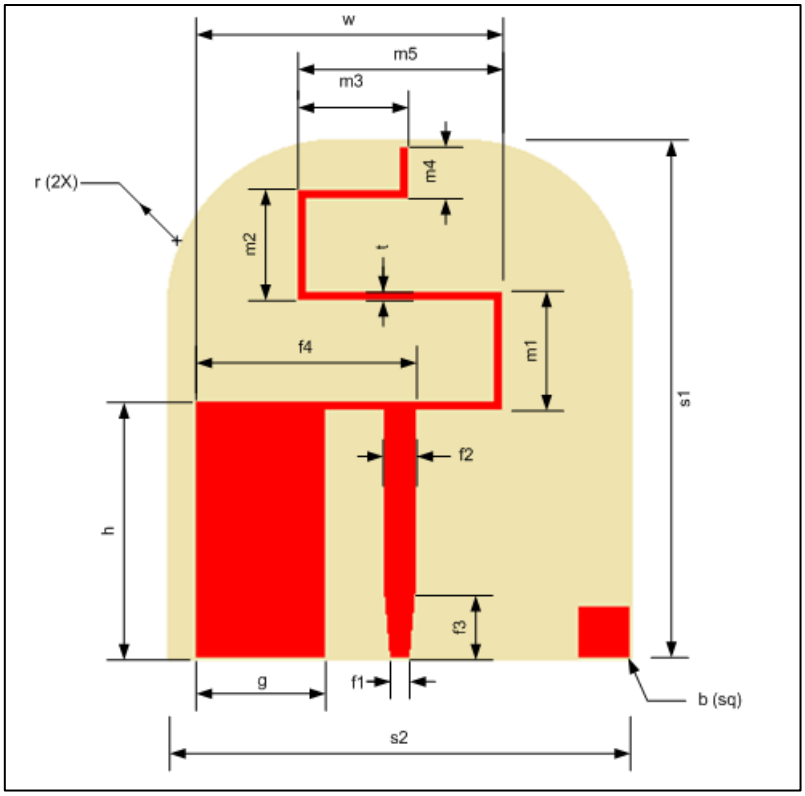

Figure 1
Designed inverted-F antenna with dimensions

Table1
Designed inverted-F antenna dimensions

Name	Value (mm)
H	10
G	5
F1	0.7
F2	1.2
F3	2.986
F4	8.55
M1	4.6
M2	4.3
M3	4.3
M4	2
M5	8
T	0.3
W	11.95
B	2
S1	20.2
S2	18
R	6.6

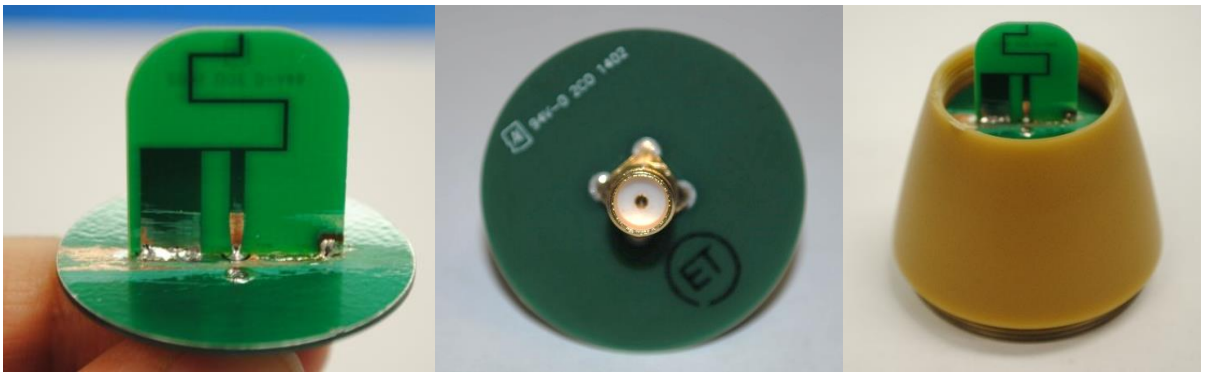

(a)
Fabricated antenna
(front view)

(b)
Fabricated antenna
(bottom view)

(c)
Fabricated antenna
and nosecone
partially assembled

(d)
Fully assembled nosecone
(front view)

(e)
Fully assembled nosecone
(bottom view)

Figure 3
The ground plane soldered to the IFA board at the ground stub and also at a small 2-mm square for mechanical support

The antenna design began as a standard inverted-F configuration with a horizontally meandered trace, a ground stub the same width as the trace, and a 5-mm separation from the ground plane. A modest bandwidth was achieved. When the width of the ground stub was increased, the ground plane separation was raised to 10 mm, the meandered trace was snaked upward, and a larger bandwidth was achieved.

ANTENNA SIMULATIONS

Simulations of the antenna were performed using Ansoft High Frequency Electromagnetic Field Simulation software (HFSS 2014) with the geometry shown in figures 4 and 5. A “discrete sweep” simulation was used for return loss plots, consisting of 200 linearly stepped points from 2 to 3 GHz. A single solution at 2.254 GHz was used for all radiation pattern plots. All geometry is surrounded by a radiation absorbing boundary condition layer. Far-field calculations are derived from a virtual radiation surface within the outer boundary. The antenna traces were modeled as thin, 20-µm thick rectangular perfect electrical conductor (PEC) volumes; the ground plane was modeled as a 30-mm diameter sheet with a PEC boundary condition with a cutout for a coaxial feed. Material properties are provided in table 2. Geometry mimicking a 50-ohm coaxial cable was included, feeding the antenna.

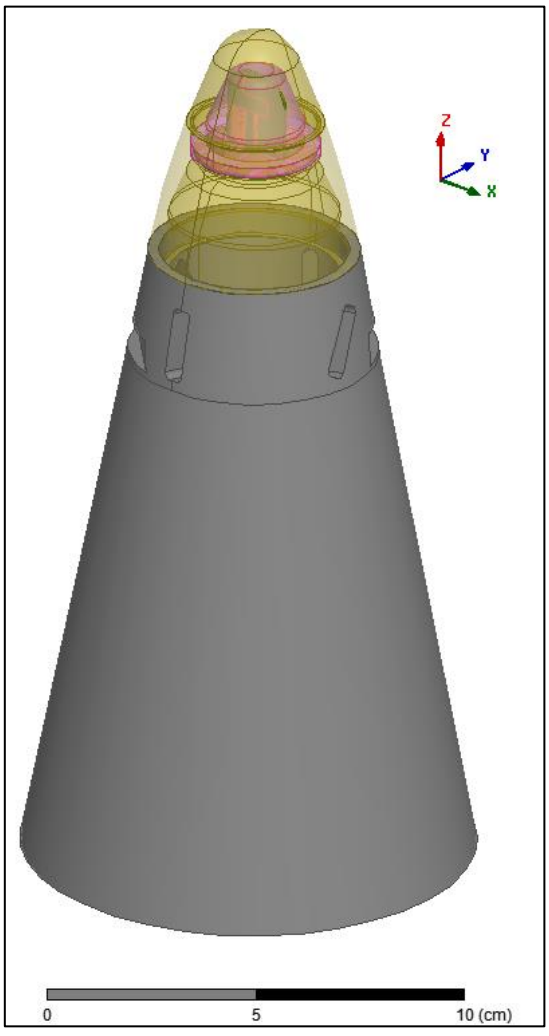

Figure 4
Simulation geometry showing upper-half of M795 body, nosecone, and antenna (isometric view)

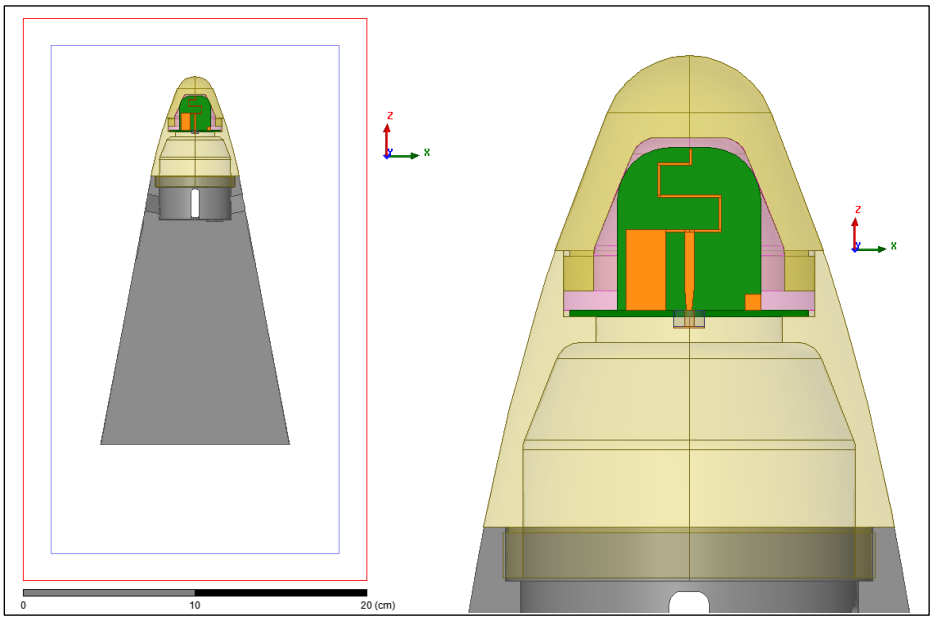

(a)
Cross section view of simulation geometry showing absorption boundary (red) and virtual radiation box (blue)

(b)
Cross section view of simulation geometry magnified on nosecone section

Figure 5
Antenna geometry modelled in Ansys HFSS 2014

Table 2
Simulation materials and associated properties

Name	Relative permittivity	Dielectric loss tangent	Relative permeability	Bulk condition (s/m)
Eccostock®	1.25	0.005	1	0
PEC	1	0	1	1e30
Teflon™	2.1	0.001	1	0
Ultem™	3.5	0.0014	1	1e-15
Vacuum	1	1	0	0

ANTENNA MEASUREMENTS

The return loss of the antenna was measured using an HP 8753E vector network analyzer (VNA). The antenna was mounted in the Ultem™ 2300 nosecone and encapsulated with the Eccostock® foam. The VNA was connected directly to the subminiature version A connector on the underside of the ground plane using coaxial cables.

The radiation pattern of the antenna was measured in an anechoic chamber (17.20 by 3.35 by 3.35 m, SFC-16 anechoic foam) with its position and orientation controlled by a Diamond Engineering measurement system model X100 turntable. Unlike the return loss tests, the antenna was mounted on the upper portion of an M795 projectile, as shown in figures 6 and 7. A metal ogive section was also included between the nosecone and half-projectile. A list of equipment used is

given in table 3. The antenna gain was derived from the measured receive power using the values and formulas shown in table 4.

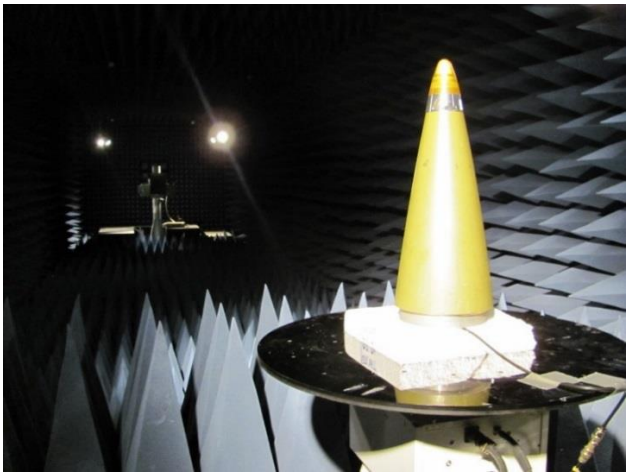

Figure 6
Anechoic chamber and M795 fixture used for radiation pattern testing, vertically positioned to measure pattern in the azimuthal plane

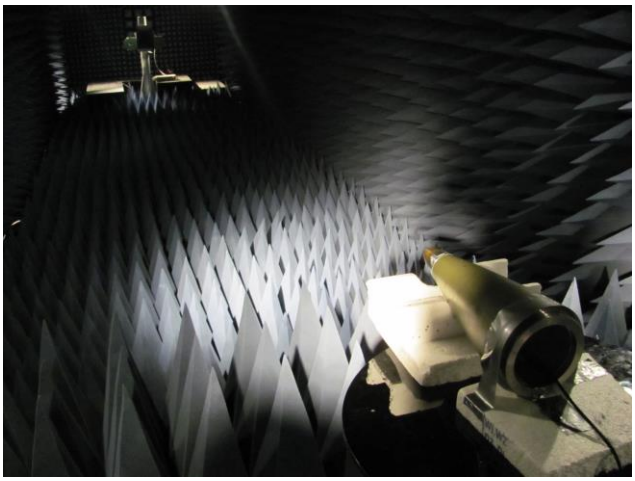

Figure 7
Anechoic chamber and M795 fixture used for radiation pattern testing, horizontally positioned to measure pattern in the elevation plane

Table 3
Anechoic chamber test equipment used

Nomenclature	Model	Serial number	Manufacturer
S-band antenna	12-1.7	353	Scientific Atlanta
Wideband amplifier	ZVA-213S+	040601239	Mini-Circuits
Power sensor	E4413A	US37181590	Agilent
Power meter	E4419A	US38260654	Agilent
Positioner table	X100	N/A	Diamond Engineering
Power supply for transmitter	E3620A	KR51301180	Hewlett Packard
Power supply for amplifier	6205C	2411A-10806	Hewlett Packard

Table 4
Gain calculation values and formulas

Name	Value	Description
f	2.254 GHz	Center frequency
Pt	0 d Bm	Transmit power
Lc	2.3 dB	Sum of cable losses
Lp	60.12 dB	Path loss
R	10.73 m	Distance between horn and antenna-under-test
Gr	16.3 dBi	Gain of horn antenna
Ga	27.50 dB	Gain of amplifier
Pr		Power received
Gt	Pr-Pt+Lp+Lc-Gr-Ga	Gain of antenna-under-test

The antenna was measured in two orientations: vertical and horizontal. Vertically oriented, the antenna was placed in the center of the turntable and spun to gather the radiation pattern in the azimuthal plane, as shown in figure 6. This pattern was measured twice, with receiver horn antenna polarized vertically (i.e., co-polarization) and horizontally (cross-polarization).

Horizontally oriented, the antenna was placed on the turntable lying flat with the axis of rotation coincident with the bottom threads of the half-M795. The antenna was supported above the table with several foam blocks, and spun to collect the radiation pattern in the elevation plane, as shown in figure 7. This pattern was measured twice with receiving horn antenna polarized horizontally (i.e., co-polarization) and vertically (cross-polarization).

ANTENNA RESULTS

Return Loss

The results of the simulated and measured return loss are shown in figure 8. The minimum measured return loss was detected at -18.89 dB at a center frequency of 2.188 GHz. The impedance bandwidth of the antenna (S11 < -10 db) was measured to be 100 MHz (4.5%), from 2.14 GHz to 2.24 GHz. This is in close agreement with the simulated return loss, which showed a minimum of -27.38 dB at 2.23 GHz (a 2% frequency error with respect to measurement) and an impedance bandwidth of 110 MHz (4.9%), from 2.18 to 2.29 GHz.

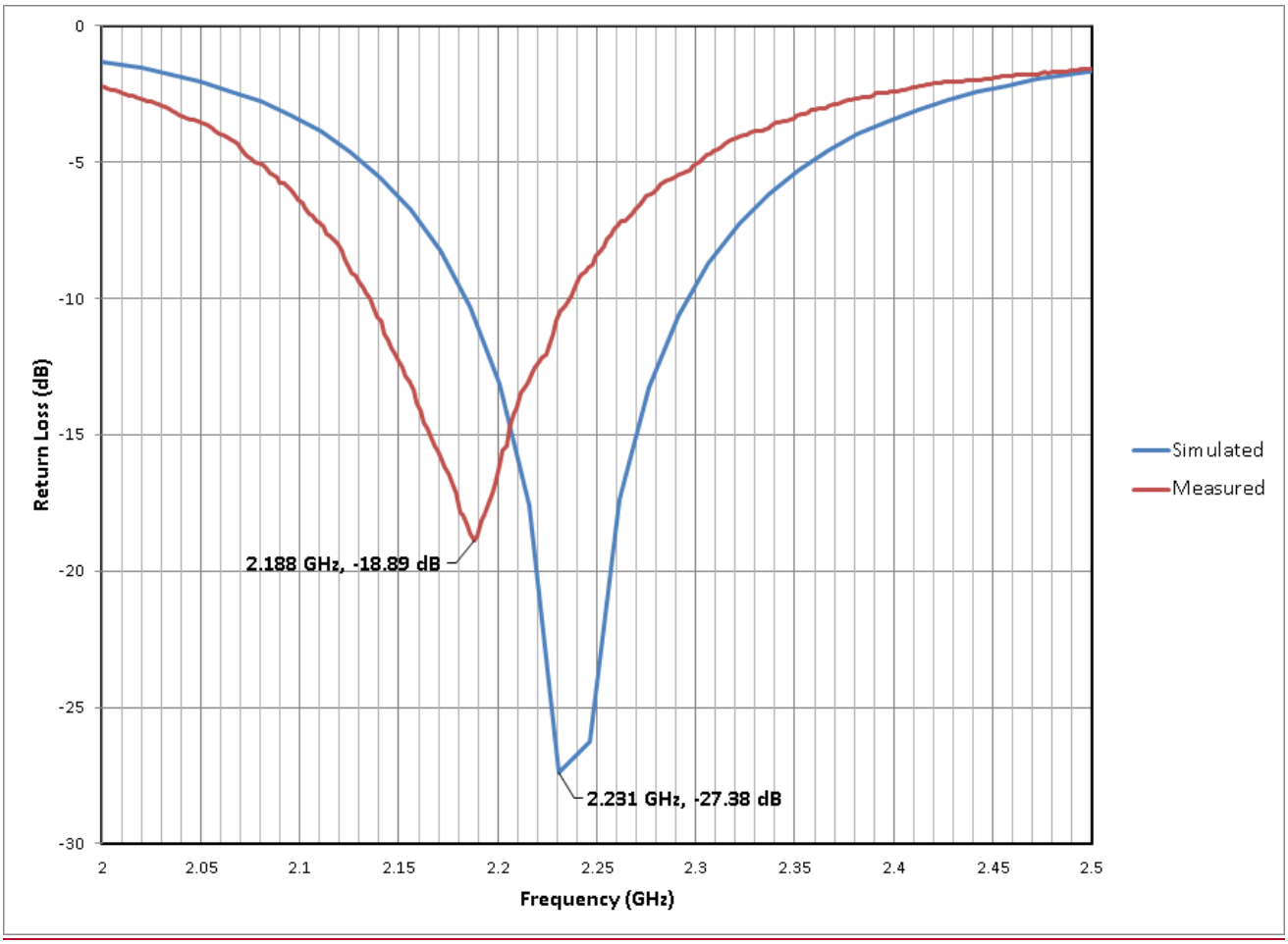

Figure 8
Measured and simulated return loss plot [S11 (db) versus frequency]

Radiation Pattern at 2.254 GHz

The antenna's radiation pattern at the intended operating frequency is generally omni-directional in the azimuthal plane. The three-dimensional (3D) renderings of the simulated radiation pattern are given in figure 9a and b. The pattern is reminiscent of that of a dipole, with two deep nulls located at the top and bottom, similar to antenna patterns shown in reference 10. Diffraction is seen to occur around the sides of the projectile, as shown in figure 10.

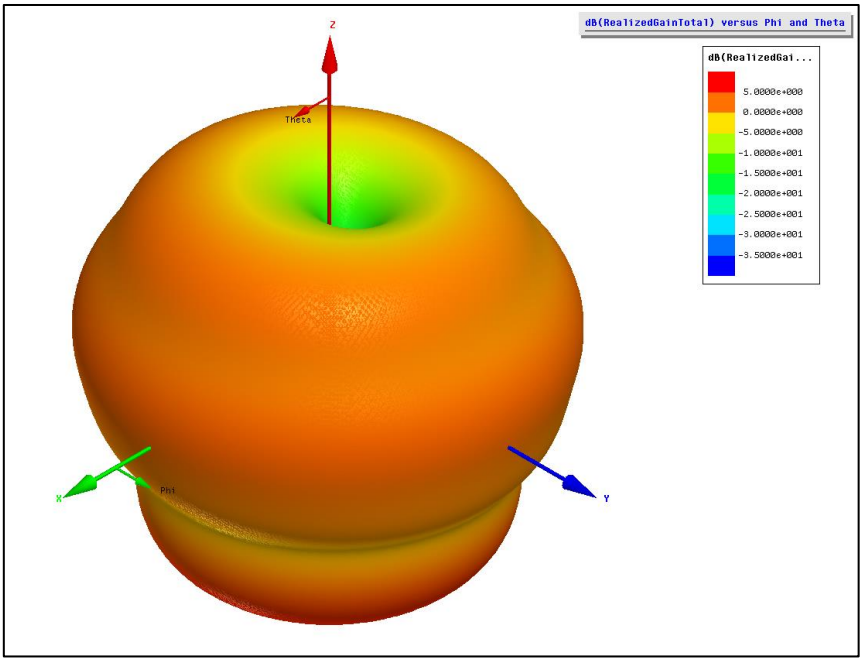

(a)
Top view

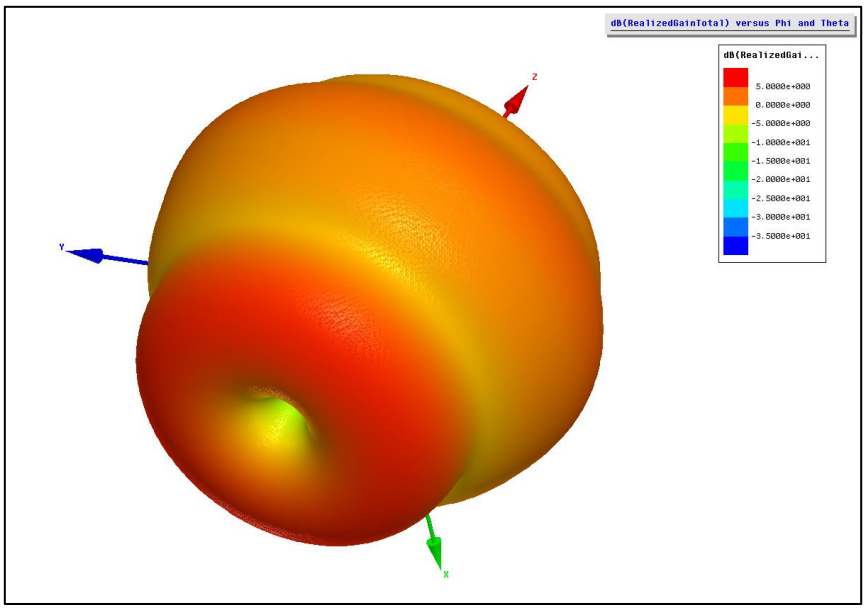

(b)
Bottom view

Figure 9
3D rendering of simulated antenna radiation pattern

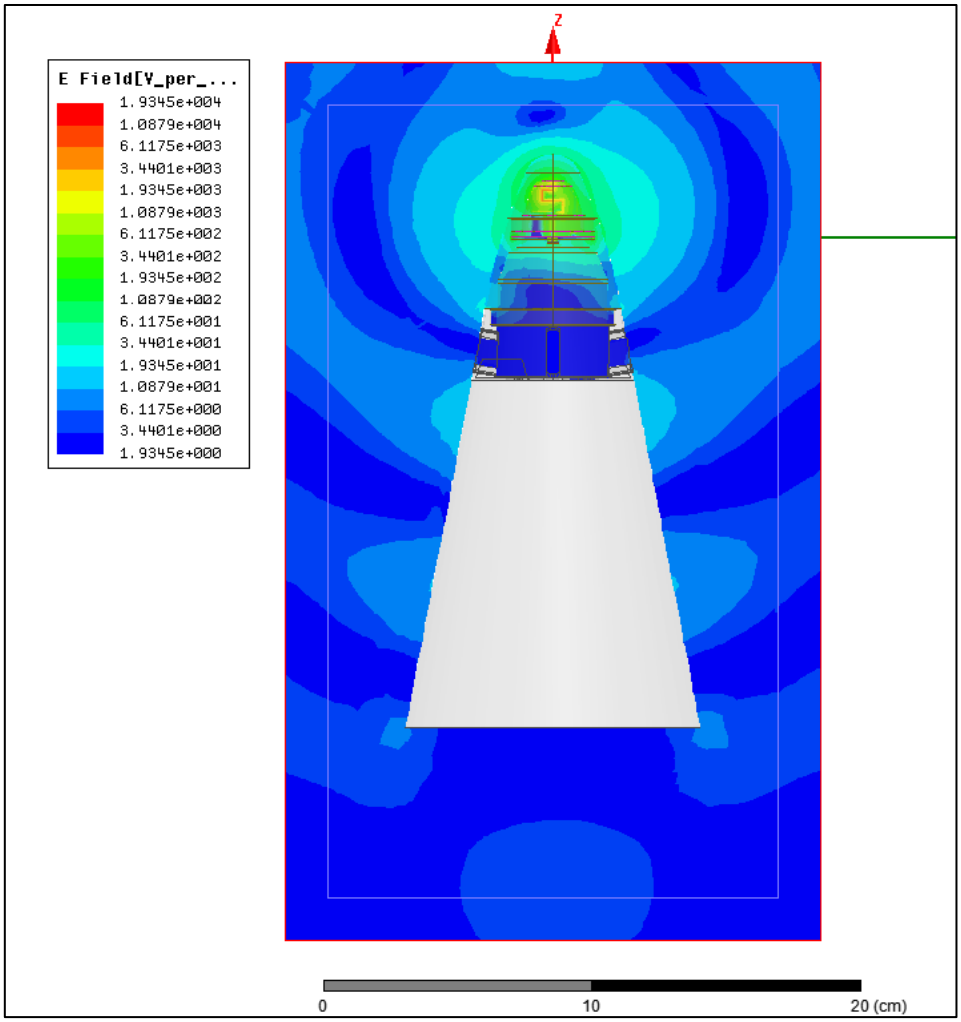

Figure 10
E-field magnitude plot in the XZ plane

The antenna's radiation pattern in the elevation plane at 2.254 GHz is shown in figure 11. The maximum gain measured was 0 dBi, with an angular coverage (herein defined as gain > -10 dBi) of approximately 150 to 170 deg, varying with the azimuthal angle. This is not in good agreement with simulation, which yielded a maximum gain of 4 dBi, with an angular coverage of approximately 161 to 168 deg. Gain is maximized toward the rear of the half-M795, and it is believed that this is due to diffraction around the metal body. Cross-polarization simulation and measurement results are shown in figure 12. A maximum measurement of -2.8 dBi was detected, as compared to a maximum simulation result of -34.7 dBi.

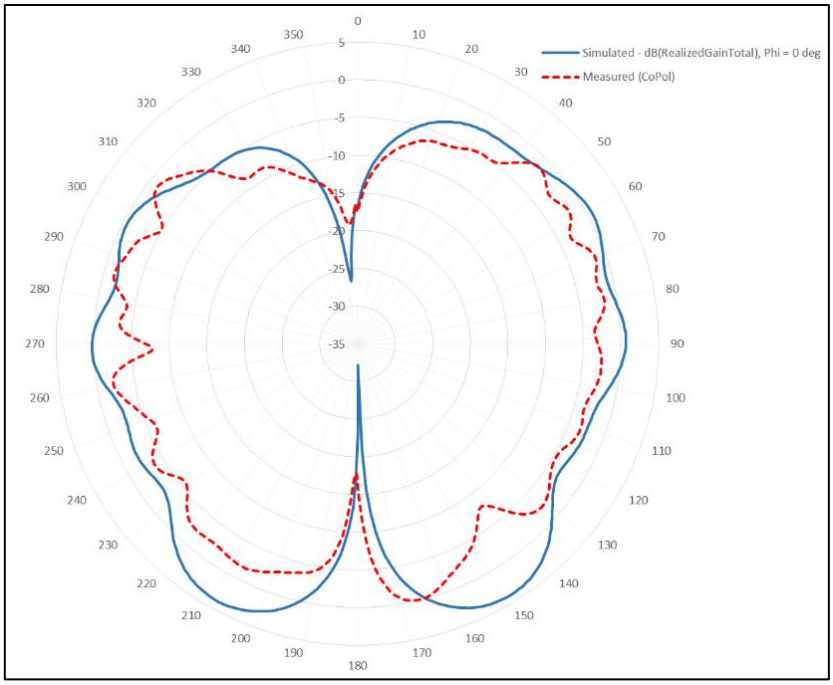

Figure 11
Measured and simulated radiation pattern at 2.254 GHz – elevation plane

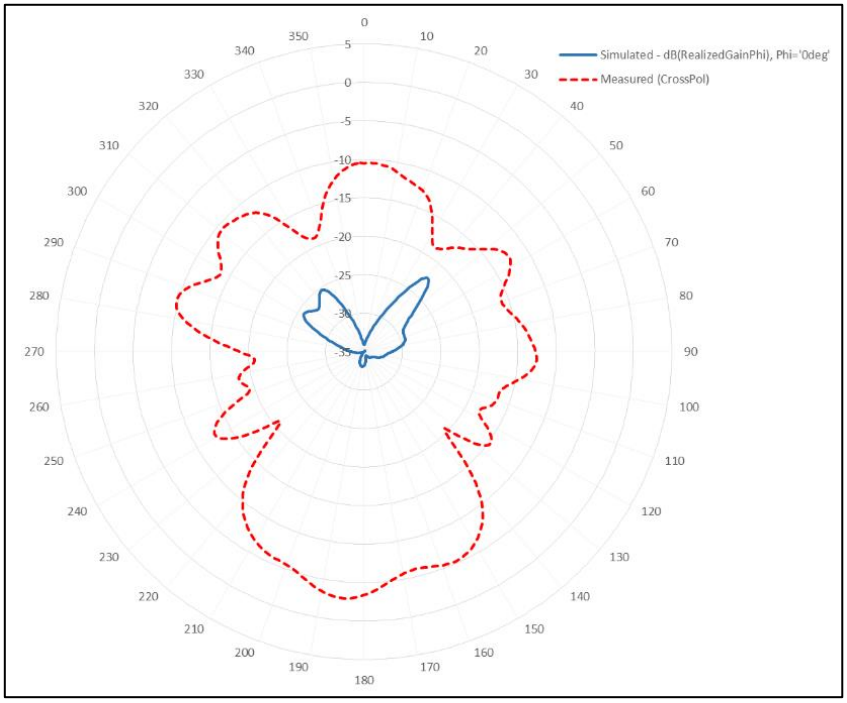

Figure 12
Measured and simulated radiation pattern at 2.254 GHz – elevation plane (cross-polarization)

The antenna's radiation pattern in the azimuthal plane at 2.254 GHz is shown in figure 13. The pattern shows excellent symmetry around the center axis, both in measurement and simulation. Cross-polarization simulation and measurement results are shown in figure 14, which yielded a maximum measurement of -13.9 dBi and a maximum simulation result of -24.1 dBi.

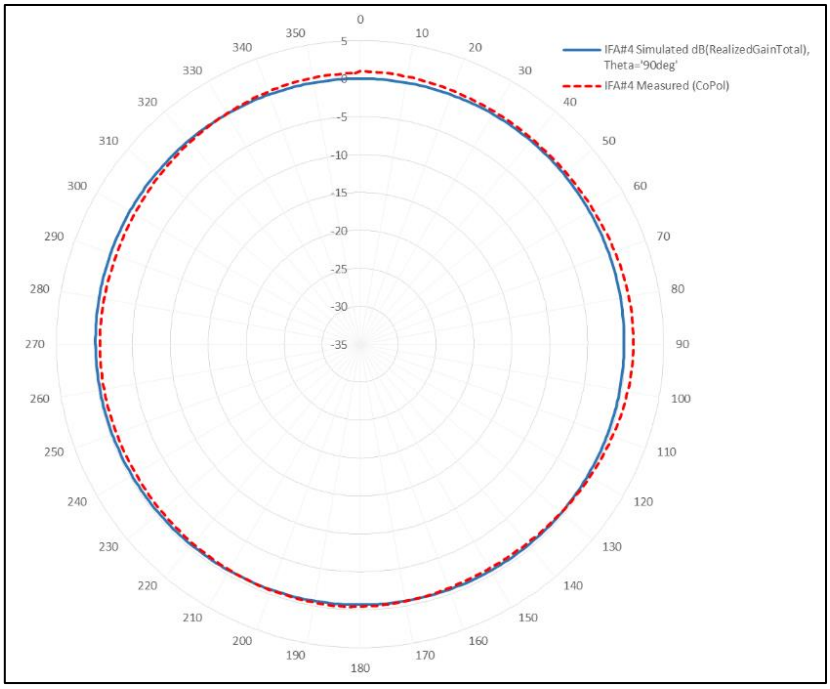

Figure 13
Measured and simulated radiation pattern at 2.254 GHz – azimuthal plane

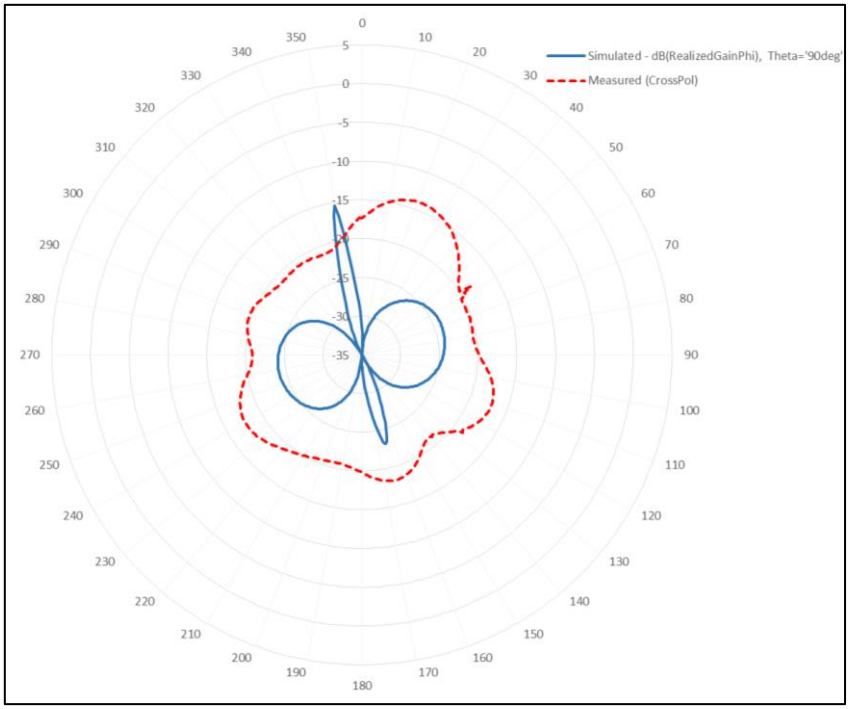

Figure 14
Measured and simulated radiation pattern at 2.254 GHz – azimuthal plane (cross-polarization)

CONCLUSIONS

The designed inverted-F antenna can be used in smart munitions for S-band telemetry. It has been fired on both 155-mm artillery and 120-mm mortar projectile platforms with success. The antenna is small, inexpensive to produce, more compact than a monopole, and requires no external matching components. It can fit underneath a plastic or any nonconductive munition nosecone. The performance of the antenna was validated by measurements in an anechoic chamber and with a network analyzer. The measurements show that the antenna operates at the intended frequency and provides omni-directional coverage azimuthally around the body of the munition.

REFERENCES

1. Pazin, L. and Leviatan, Y., “Inverted-F Laptop Antenna with Enhanced Bandwidth for Wi-Fi/WiMAX Applications,” IEEE Transactions on Antennas and Propagation, Vol. 59, no. 3, pp. 1065-1068, 2011.

2. Munson, R.E., “Conformal Microstrip Antennas and Microstrip Phased Arrays,” IEEE Transactions on Antennas Propagation, Vol. AP-22, No. 1, pp. 74-78, 1974.

3. Reggia, Frank and Jones, Howard, Jr., “Very Thin (wrap-around) Conformal Antenna,” Patent, Grant US4110751, August 29, 1978.

4. Katulka, G., Hall, R., Topper, B., and Hundley, N., “Design and Analysis of Embedded Antennas for 60-mm Mortars,” Technical Report ARL-TR-4483, U.S. Army Research Laboratory, Aberdeen Proving Ground, Aberdeen, MD, June 2008.

5. Grzybowski, David M., Peregino, Philip J., and David, Bradford S., “Development of a Telemetry-Enabled High-G Projectile Carrier,” Technical Report ARL-TR-6099, U.S. Army Research Laboratory, Aberdeen Proving Ground, Aberdeen, MD, September 2012.

6. Farr, David and Henderson, William, "Airborne Antenna Considerations for C-Band Telemetry Systems,” Haigh-Farr, Inc., Bedford, NH, October 2014.

7. Ryken, Marvin Jr. and Davis, Albert, "TM Microstrip Antenna with GPS Frequency Coverage," Patent, Grant US7193567 B1, March 20, 2007.

8. Ryken, Marvin Jr. and Davis, Albert, "Broadband Telemetry Antenna Having an Integrated Filter," Patent, Grant US6630907 B1, October 7, 2003.

9. Microcom Corporation, Scimitar Antenna Model AT-5.

10. Katulka, Gary and Hall, Rex, "Electro-Dynamic Analysis of 60mm Mortars Modified with Guidance, Navigation, and Control Components," IEEE Antennas and Propagation Society International Symposium, pp. 1-4, Toronto, ON, 2010.

DISTRIBUTION LIST

U.S. Army ARDEC
ATTN: RDAR-EIK
RDAR-MEF, D. Troast
F. Loso
RDAR-MEF-E, J. Cordes
RDAR-MEF-I, A. Barton
C. Sandberg
P. Sweeney
R. Granitzki
Picatinny Arsenal, NJ 07806-5000

Defense Technical Information Center (DTIC)
ATTN: Accessions Division
8725 John J. Kingman Road, Ste. 0944
For Belvoir, VA 22060-6218

U.S. Army Research Laboratory
ATTN: RDRL-WML-F, B. Davis;
T. Harkins
M. Don
R. Hall
Aberdeen Proving Ground, MD 21005-5069

U.S. Army Research Laboratory
ATTN: RDRL-SER-M, S. Weiss;
T. Anthony
W. Coburn
A. Zaghloul
Adelphi, MD 20783-1138

GIDEP Operations Center
P.O. Box 8000
Corona, CA 91718-8000
gidep@gidep.org

REVIEW AND APPROVAL OF ARDEC TECHNICAL REPORTS

Nosecone Inverted-F (IFA) Antenna for S-band Telemetry

Title

Date received by LCSD

Aaron Barton

Author/Project Engineer

Report number (to be assigned by LCSD)

x3521 95

Extension Building

Precision Munitions Instrumentation Division

Author's/Project Engineers Office
(Division, Laboratory, Symbol)

PART 1. **Must be signed before the report can be edited.**

a. The draft copy of this report has been reviewed for technical accuracy and is approved for editing.

b. Use Distribution Statement A ✓, B___, C___, D___, E___, F___ or X___ for the reason checked on the continuation of this form. Reason: _____

1. If Statement A is selected, the report will be released to the National Technical Information Service (NTIS) for sale to the general public. Only unclassified reports whose distribution is not limited or controlled in any way are released to NTIS.

2. If Statement B, C, D, E, F, or X is selected, the report will be released to the Defense Technical Information Center (DTIC) which will limit distribution according to the conditions indicated in the statement.

c. The distribution list for this report has been reviewed for accuracy and completeness.

Craig Sandberg

Division Chief

26 MAY 2016
(Date)

PART 2. To be signed either when draft report is submitted or after review of reproduction copy.

This report is approved for publication.

Craig Sandberg

Division Chief

11 SEP 2017
(Date)

Andrew Pskowski

RDAR-CIS

9/14/17
(Date)

LCSD 49 supersedes SMCAR Form 49, 20 Dec 06